Evolution of spectral power density in grounded-cathode relativistic magnetron

Itzhak Schnitzer, Avner Rosenberg, Chaim Leibovitch, I. Cohen, M. Botton, et al.

Itzhak Schnitzer, Avner Rosenberg, Chaim Leibovitch, I. Cohen, M. Botton, J. Leopold, "Evolution of spectral power density in grounded-cathode relativistic magnetron," Proc. SPIE 2843, Intense Microwave Pulses IV, (28 October 1996); doi: 10.1117/12.255399

SPIE.

Event: SPIE's 1996 International Symposium on Optical Science, Engineering, and Instrumentation, 1996, Denver, CO, United States

Evolution of spectral power density in grounded cathode relativistic magnetron

I. Schnitzer, A. Rosenberg, C. Leibovitz, I.Cohen, M. Botton, and J. Leopold

Rafael, Department #23, P.O.Box 2250, Haifa 31021, Israel.

FAX:+972-4-897-5315. E-mail: Schnit@Netvision.Net.il

ABSTRACT

A novel, rep-rated, relativistic magnetron design is demonstrated. Unlike other relativistic magnetrons, the high voltage pulse is positively charged, feeding the anode block, while the cathode is grounded. Moreover, the anode-cathode interaction space is centered in a larger *buffer* cavity that serves as an electric insulator and electromagnetic impedance matching between the anode block and the exit waveguide(s). The grounded cathode geometry eliminates the axial current (improving efficiency) and enables the use of compact, CW, U-shaped electromagnet. It may also be utilized for frequency tunability through the buffer cavity in a way similar to coaxial magnetrons. Operation with peak power of 50MW (100MW) and pulse length of 150ns (70ns) has been achieved. Employing metal-dielectric cathodes led to repetitive operation up to 10Hz. The analysis emphasizes time-resolved spectral power density of both in-cavity and emitted microwaves in regard to the undesirable occurrence of pulse shortening.

Keywords: relativistic magnetron, high-power microwaves, metal-dielectric cathode, time-frequency distribution, pulse shortening, magnetron cavity design

1. INTRODUCTION

Since the first landmark by Bekefi et al.,[1] announcing the *A6* relativistic magnetron, substantial improvements accomplished peak power levels of several gigawatts. However, pragmatic considerations emphasized repetitive mode of operation and longer pulse duration (i.e., higher average power) at the expense of peak power. Repetition rate of about 200pps with peak power levels around 600MW and pulse lengths 30ns (~20J/pulse) were achieved by Physics International, USA,[2,3] and 360MW/60ns (~22J/pulse) by the Institute of Nuclear Physics, Tomsk, Russia.[2,4]

Further progress seems to be impeded by the following two facts: *i)* Both of these leading groups, which employ versions of the A6 resonator geometry, confront with an underlying limitation of the pulse energy, also known as *pulse shortening*. *ii)* The required magnetic field coils are either too large for numerous applications (PI's at CW operation), or, if suitably smaller, can be operated only in short bursts.[4]

At *Rafael*, we recently initiated a relativistic magnetron program that emphasizes compactness and repetitive operation at longer pulse duration (~200ns) with pulse energy > 20J. To fulfill these requirements we explore a new design, named hereafter as the *grounded cathode magnetron*. This paper presents the design considerations of the new geometry, some preliminary results, and physical interpretations of the measured time-resolved spectral power density.

2. DESIGN

2.1 Grounded Cathode Geometry

Our magnetron design (Patent pending) is fundamentally different from the above mentioned relativistic magnetrons. As shown in Figure 1, the cathode is grounded and the positive high-voltage

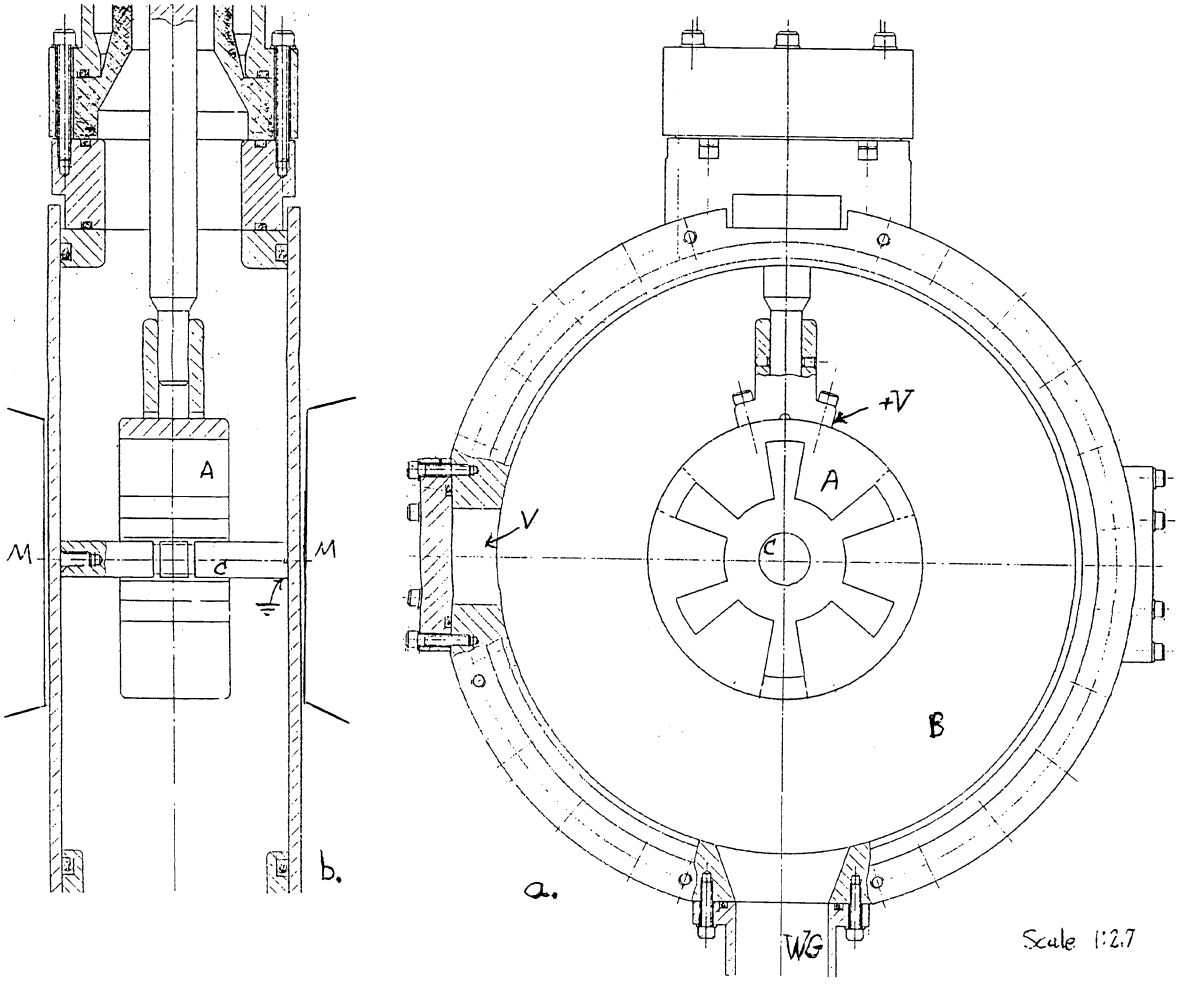

Figure 1. Grounded Cathode Magnetron design, top view is (a) and side view (b). Note the anode block (A), the cathode (C), the buffer cavity (B), the electromagnet poles (M), the waveguide exit (WG), the pumping port (V), and the ceramic interface (darkened) with the transmission line.

(H.V.) pulse is injected to the anode block (essentially, an A6 resonator). The anode block is centered in a cylindrical cavity, the *buffer cavity*, which isolates the positively charged anode from the buffer cavity walls, the exit waveguide, and the transmission line. Note that the buffer cavity diameter is 210mm and **84mm wide** (90mm externally) accommodating an A6 resonator operating around 2.5GHz.

Injecting a positive pulse through a buffer cavity has the following major advantages:

1. The H.V. transmission line is connected perpendicularly to the DC magnetic field axis. Such a configuration enables the use of a compact U-shaped electromagnet instead of the large Helmholtz coils that are often used in relativistic magnetrons. See the side view in Figure 1.
2. There are no axial currents in the grounded cathode geometry since both the surrounding walls and the emitter are at the same potential. The elimination of the axial current component improves the electronic effeciency since all the electrons fall to the anode block.
3. The external cavity functions as a buffer between the anode-cathode (A-K) interaction region and the output waveguide. In other words, the buffer cavity can be regarded as an electromagnetic impedance matching element that reduces the stored energy density for the same output power.
4. The grounded cathode magnetron may be tunable through the buffer cavity in a way similar to coaxial magnetrons. Alternatively, broad tunability range may be achieved by a mechanical change of the **grounded** cathode dimensions in a way similar to the anode regulation implied by the PI group.[5]
5. The grounded cathode scheme is most suitable for the employment of more sophisticated and innovative, long lifetime, emitters such as plasma cathodes. The option of timed cathode excitation by another low (-) voltage trigger electrode seems very promising.
6. There is an inherent advantage in transmitting a positively charged H.V. pulse as opposed to a negatively charged pulse. Generally speaking, it allows for tighter lines for equivalent charging.

One disadvantage of the grounded cathode geometry is the control of electrons ejected from the buffer cavity walls toward the anode block and feed line, and of positive ions traversing the buffer cavity. Another difficulty is the electromagnetic cavity design which is generally more demanding because of the crucial role played by the external (buffer) cavity and its coupling to both the A-K resonator and the waveguide. These drawbacks are presently contemplated as will be described later.

2.2 Metal-Dielectric Cathode

We have attempted many of the conventional cathode designs including edge-enhanced metallic cathode, velvet cathode, and graphite. However, none of these were found suitable for **repetitive,** relatively **low voltage** (<300kV), and **large gap** (14mm) as imposed by our magnetron design. They were either emission limited or rep-rate limited.

Introducing compound cathode design, particularly the metal-dielectric cathode (MDC), yield significant improvements. In MDC, best described by Mesyats and Proskurovsky,[6,7] the surface microexplosive process that develops into a self-sustained explosive electron emission (EEE) is initiated in the so called **triple points** (metal-dielectric-vacuum interface). This emission mechanism, enhanced

by the dielectric material ($\varepsilon > 1$) presence, was known for a long time as a clean (in terms of vacuum integrity), high current density, low voltage, and long lifetime source.

So far we have used uncontrollable MDC schemes. The emissive section of a typical cathode is 20mm long, centered at the mid-plane of the 40mm thick anode. It consists of alternating disks of metal and dielectric materials. Some of the metallic disks are floating (electrically) and their diameter, thickness, sharpness, and composition are varied in order to optimize the emission characteristics. In this scheme, capacitive links through adjacent metallic disks result in strong surface fields at the triple points which later develop to surface plasma over the dielectric disks from which electrons are being extracted by the positively charged anode.

Although such simple MDC seem promising, we feel that there is still a lot to improve. It is both technologically valuable and physically interesting to master the dimensions and material science that determines emission time scale, uniformity, and cathode longevity. We are presently looking to contract the apparent emission delay (> 20ns) which lowers the overall efficiency. In the future, we may include controllable MDC by a special trigger electrode (-5kV, roughly) to initiate the surface plasma prior to the H.V. pulse.

3. OPERATION

3.1 Diagnostics

We use several field probes, simultaneously. Typically a far-field probe/antenna, one small loop in the buffer cavity, and one at the exit waveguide. Each of these RF signals is attenuated and split into three channels: one into a Schottky diode detector (power envelope), and two are being mixed with local oscillators (LO) set at two different frequencies (upper LO & lower LO). The diode current and voltage traces are recorded as well. Other diagnostic tools, such as Ne lamp arrays and open shutter photography (time integrated), are also valuable.

All this data has been recorded for several cathode types and different anode and buffer cavity designs. Here we only emphasize the study of the emitted spectral power density as a diagnostic tool.

3.2 Time-Resolved Spectral Power Density

Typical pulse length is about 200ns, as shown in Figure 2. Sampling of these pulses at rates of 1Gs/second, as we do, can reveal not only their spectral content but also their time evolution with acceptable resolution. The temporal evolution of the trace from Figure 2 is shown in Figure 4.

The most natural thing to do is to divide the signal into overlapping segments and to find the spectral power density of each segment (temporal window). That procedure is known as *running window,* or *Gabor transformation.* When squared to yield the power density it is known as *spectrogram.* Mathematically, the time resolved spectral power density, of the signal S(t) is given by[8]

$$P_{SPEC}(t,\omega) = \left| \int \exp(-i\omega t')S(t')h(t'-t)dt' \right|^2$$

where h(t) is a carefully chosen smoothing window function. This relatively simple transformation was found to be problematic for signals whose frequency varies significantly within each time segment. It also tends to peak artificially at the window center. Consequently, we were looking for more sophisticated time-frequency distributions using adaptive window size that is optimized to the temporal signal behavior. In particular, the class of *Orthonormal Shift-Invariant Trigonometric Decomposition.*[9] We have learned that none of these linear transformation gave reliable picture of the time-resolved spectral power.

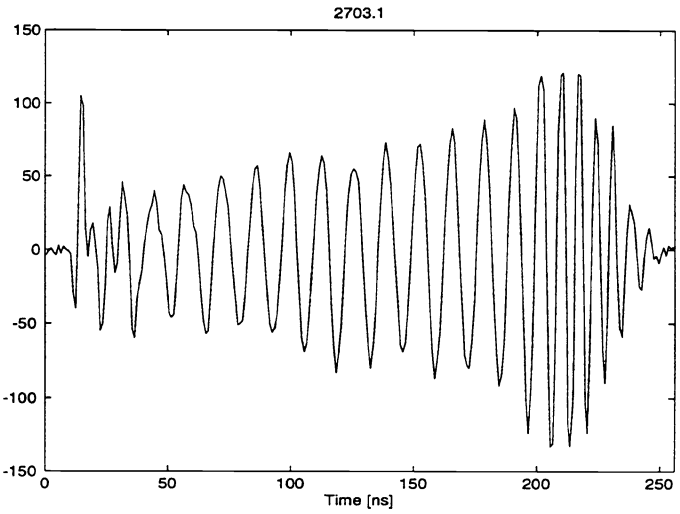

Figure 2. Heterodyne signal sampled at 1GS/s (RF – LO)

However, it was found that Cohen's class smoothed distributions are more reliable for these short pulses. Of these, the most known is the *Wigner* distribution defined as

$$P_W(t,\omega) = \int S^*(t-\tau/2)\exp(-i\omega\tau)S(t+\tau/2)d\tau.$$

The main disadvantage of such bilinear transformation is the artificial cross terms resulting from interfering distinct components in the time-frequency plane. That problem was minimized by a proper smoothing function with an acceptable loss of T-F resolution. The data which is presented here was processed by the following *Smoothed Pseudo Wigner* distribution (SPW).

$$P_{SPW}(t,\omega) = \int \sqrt{\alpha\beta}\,\exp\left[-\alpha(t-t')^2 - \beta(\omega-\omega')^2\right] P_W(t',\omega')\,dt'\,d\omega'$$

where the smoothing parameters α and β were optimized for the type of measured traces that we have and remain unchanged throughout the analysis.

3.3 Mode Competition and Chirping

Figure 3 presents the time-resolved spectral density for a magnetron operated with a velvet cathode in a single-shot mode with B_{axial} = 2.1kG. In 3a, the averaged diode voltage (on the plateau) and current were V = 220kV and I = 0.7kA, and the emitted peak power was 50MW. (In all cases the radiation was emitted through a circular waveguide into a conical antenna and measured with a calibrated antenna placed in the far field.). In 3b we measured V = 180kV, I = 1.4kA, and the emitted peak power was 100MW.

The two central frequencies, or modes, in Figure 3 seem quite reasonable in light of the fact that the computed[10] eigenfrequency of the $2\pi/3$ mode and the π mode are 2.424 GHz and 2.518 GHz, respectively. Moreover, it looks as if the $2\pi/3$ mode builds up faster due to the higher voltage at the

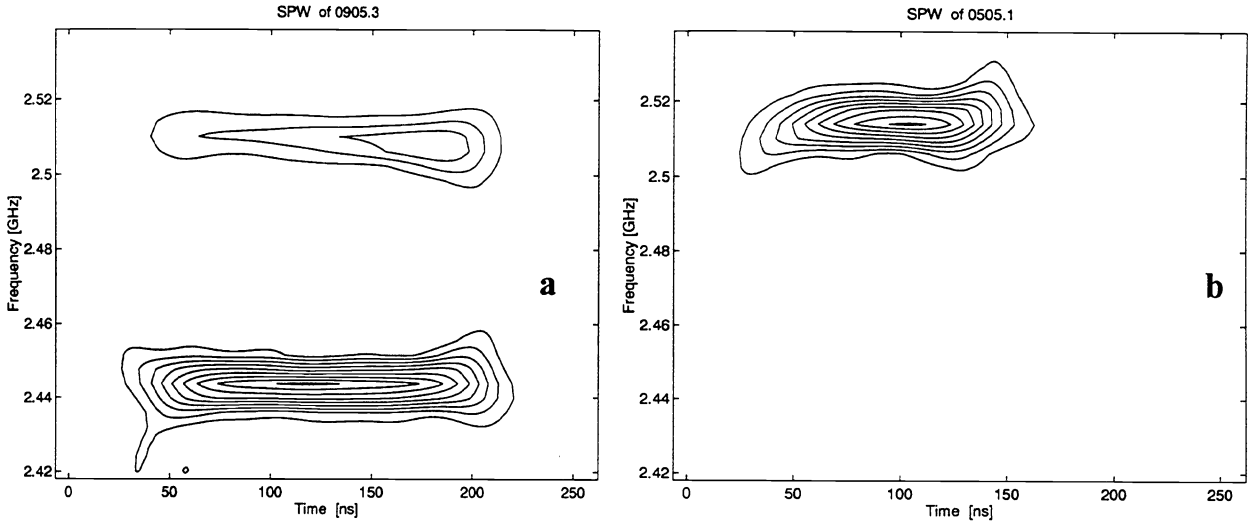

Figure 3. Time-resolved spectral density from the magnetron. Details are given in the text above.

beginning of the pulse and then, as the impedance (and voltage) drops, the electron drift velocity tends to synchronize with the π mode. This mode competition reduces the efficiency which otherwise is expected to be as high as 50% in the absent of axial currents.

At slightly higher charging, and perhaps more effective, under different vacuum conditioning, we managed to reduce the diode impedance to about 120Ω (matched to the generator), as in 3b. Indeed, under these conditions we see single mode (π) efficient operation, in accordance with the Hull/Bunneman-Hartree V - B plane. However, the microwave pulse terminates after about **70ns**. In fact, when examining the evolution of the in-cavity spectral density we find it to be pronounced in the $2\pi/3$ mode just prior to the build up of the externally emitted π mode. Such perplexing observations are quite common but were not quantified because of the unknown coupling of each mode to the internal field probe. They attest, however, on the existence and timing of other modes in the buffer cavity.

As a last example of this section we examine the temporal evolution of the spectral power density obtained with a preliminary design of MDC. The emission dynamics of this cathode is noticeably different from the previously described velvet cathodes, as shown in Figure 4. Instead of specific mode signature we observe frequency **chirping** (not always with a knee shape, in some cases it evolves along diagonal lines in the T-F plane). It is believed that the chirp develops due to cathode

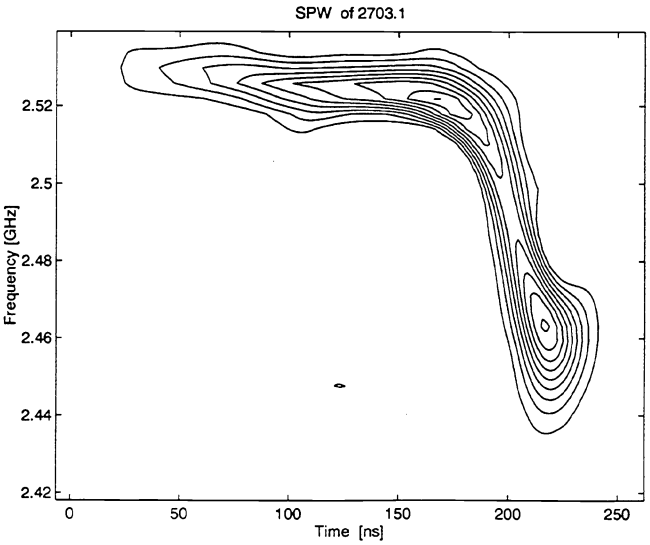

Figure 4. Chirped magnetron emission with MDC.

plasma motion outward which effectively increases the cathode diameter. Calculation shows that as the cathode radius expands from 8mm to 13mm, the π mode frequency changes from 2.518 GHz to 2.465 GHz for anode inner and outer radii of 22mm and 42mm, respectively, as we have.

3.4 Pulse Shortening

At this point we note the following observations with regard to the pulse shortening: *i)* Square 150ns flat top pulses with single mode frequency of 2.52 GHz were routinely observed, but in these cases the peak power was under 36 MW. *ii)* In all cases of pulse shortening (Figure 3b. and 5b. below) the emitted power was single moded, within the emission band width of about 15 Mhz. *iii)* Open shutter photography through the exit waveguide, vacuum window, and the anode coupling slot, did not reveal any specific record of pulse shortening (internal breakdowns are clearly evident).

Of the possible explanations that we have considered, it seems that plasma gap closure, either anode or cathode plasmas, is unlikely due to the steady spectral content of these pulses. The plasma motion should change the RF boundary and thereby chirp the resonant frequency as shown in Figure 4. Excluding RF breakdown as the cause for pulse shortening, based on our in-cavity photography, is less certain. However, the mere fact that we also experience pulse shortening at lower power density compare to other groups indicate that it is of a more universal nature and should be looked for elsewhere.

In light of the above mentioned observations, the fact that our magnetron impedance is typically larger than that of the generator's, and the predominant role of the cathode emission mechanism, we believe that **impedance mismatch** is to be blamed for pulse shortening. The term impedance mismatch should be taken in a generalized manner to include both the electrical impedance and the electromagnetic impedance since they are strongly coupled. In an oscillator, the load conductance (RF out-coupling) determines the electrical load, which in turn determines the voltage, the electrical power, pulls the frequency (or pushes for purely resistive load), and so on, in a self consistent manner. This interplay is governed by the cavity Q factors, out-coupling factor, and through the specific dependence of the diode complex impedance on the applied voltage. In magnetron theory, it is customary to present this interplay in Rieke diagrams in which contours of constant power and of constant frequency are drawn in the load admittance plane. Such Rieke diagrams,[11] can explain how impedance mismatch may lead to pulse shortening.

3.5 Repetitive Operation

At first, the MARX-PFN generator was upgraded to produce nearly square pulses of up to 300kV on matched impedance of 120Ω at the rate of 10pps. The magnetron was then operated using a metal-dielectric cathode (MDC-1) as mentioned above in relation to Figure 4. Although, repetitive operation was successful, the cathode emission was poor. In order to improve the emission (and reduce the cathode plasma), the design was revised (MDC-2) as described in 2.2 above. These new cathodes are thicker than the former and therefore lower resonant frequency are expected.

Figure 5 presents two examples of pulse bursts as analyzed by a spectrum analyzer (note, power is measured in dBm). In the first case (5a), a burst of about 250 pulses at 5pps and peak power around 40MW was scanned for 50 seconds with 2MHz band width. As expected the main frequency is indeed lower. However, this shift is much too large and is excused, for the moment, by structural asymmetry. Note that coexist with the main emission frequency at 2.28GHz is the component at 2.518 GHz, about 6dB lower. Note also that that the density of lines implies that misfire is rare if not absent.

Figure 5b is similar but was recorded at full charging voltage for a shorter time (20s). The rate was 5pps as well and the peak power around 65MW. The main difference between the two bursts is, however, the absence of the higher frequency component in the second burst. We should point out that pulses form the more intensed burst were short, about 70ns, while those shown in Figure 5a varied in pulse lengths between 70ns to 150ns. Similarly, we recorded the spectra from the internal field probe and found it to resemble the emitted one in both cases.

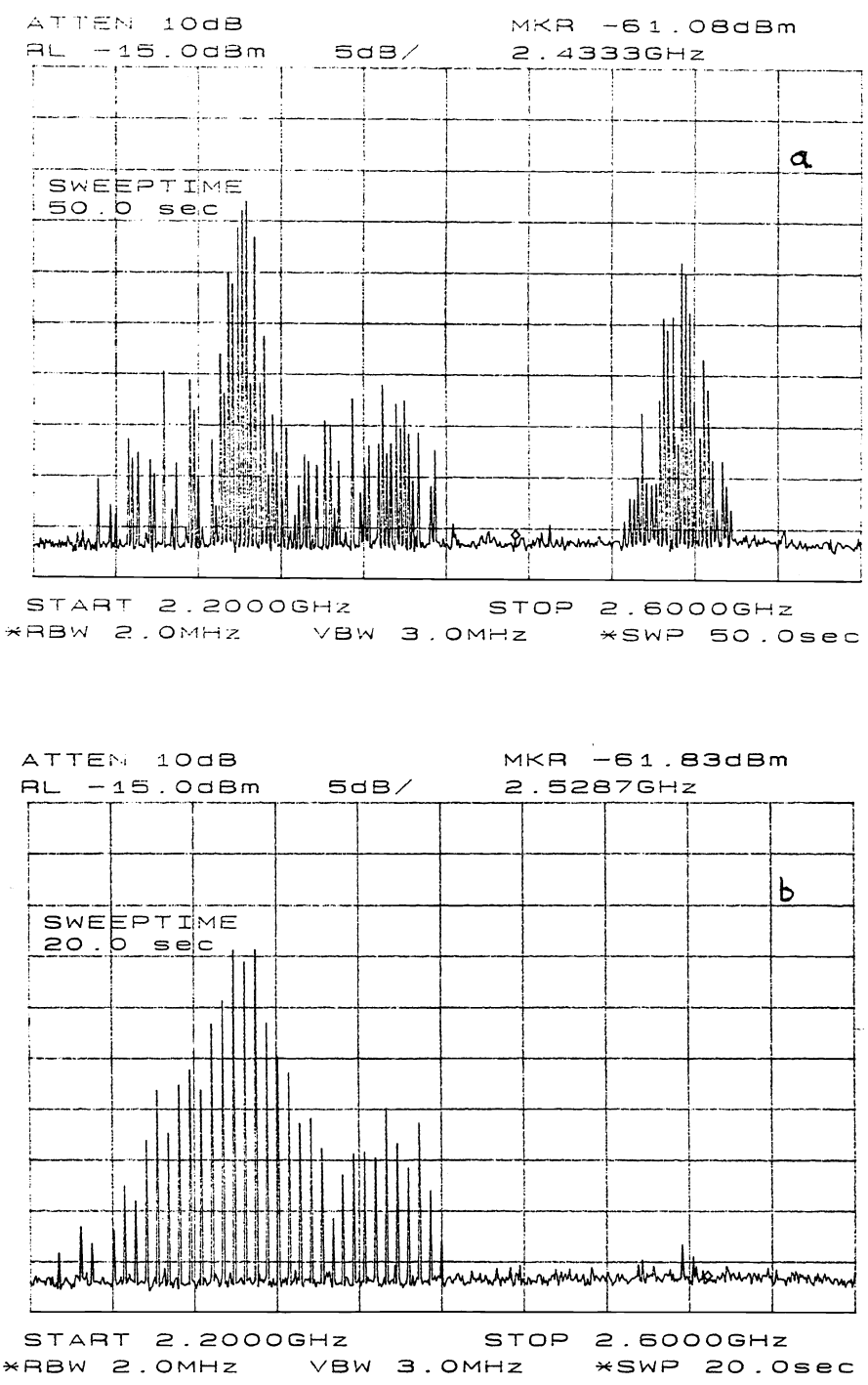

Figure 5. Burst mode operation of the magnetron at 5pps as recorded by a spectrum analyzer at 2MHz band with for 50 second (**a**.on top) and for 20 seconds (**b**. on the bottom). In both cases the emitted main frequency is 2.3GHz, and peak power is 40MW in **a** and 60 MW in **b**. Note the absence of the higher frequency component in the more intense burst.

4. SUMMARY

We have described a novel relativistic magnetron design which is fundamentally different from other relativistic magnetrons. The *grounded cathode* geometry eliminates axial current, allows the use of a more compact electromagnet, incorporates a buffer cavity to achieve better adaptivity (and complexity) to intense RF fields, and is more permissible to advanced rep-rated cathode designs.

We emphasized the capacity of time-resolved spectral analysis as an important diagnostic tool. It led us to the conclusion that pulse shortening is most likely due to impedance mismatch. We believe that it should be challenged by adapting the diode impedance characteristics (cathode dynamics) to the electromagnetic load. Presently, we are in the process of full 3D electromagnetic simulation (EMA3D code, Electromagnetic Applications, Inc., Denver) of the complete structure including the resonators, the buffer cavity, and the exit waveguide.

Metal-dielectric cathodes were found to be promising for such low voltage, rep-rated, relativistic magnetron. They performed almost as good as the simple (single shot) velvet cathodes at rates of 10pps. We feel that there is still a lot to improve in MDC design. With the *grounded cathode* it is also tempting to think of more innovative cathode schemes for better impedance matching.

5. REFERENCES

1. A. Palevsky and G. Bekefi, "Microwave emission from pulsed, relativistic E-beam diodes," *Phys Fluids*, **22**, 985, (1979), and G. Bekefi and T. J. Orzechowski, *Phys. Rev. Lett.* 37, 379 (1976).
2. J. Benford and J. Swegle, High-Power Microwaves, Artech house, 1992.
3. R. Smith, J. Benford, N. Cooksey, N. Aiello, J. Levine, and B. Harteneck, "Operation of an L-band relativistic magnetron at 100Hz," *Intense Microwave & Particle Beams II,* ed H. Brandt, *SPIE*, **1407**, 83 (1991).
4. V. V. Vasil'yev, I. I. Vintizenko, A. N. Didenko, Y. I. Lukonin, A. S. Sulakshin, G. P. Femenko, and E. G. Furman, "Relativistic magnetron operating in the mode of a train of pulses," *Sov. Tech. Phys. Lett.*, **13**, 762, (1987).
5. J. S. Levine, B. D. Harteneck, and H. D. Price, "Frequency agile relativistic," *Intense Microwave Pulses III,* ed H. E. Brandt, *SPIE*, **2557**, 74 (1995).
6. A. Mesyats, "Physics of electron emission from metal-dielectric cathodes," *BEAMS '94* pp. 93-99.
7. A. Mesyats and D. I. Proskurovsky, Pulsed Electrical Discharge in Vacuum, Springer Series on Atoms & Plasmas, Springer-Verlag , Berlin, 1989.
8. Cohen, "Time-frequency distribution - a review," *Proceedings of the IEEE* **70**, 941-981 (1989)
9. Cohen, S. Raz, and I. Schnitzer, "Best basis algorithm for orthonormal shift-invariant trigonometric decomposition," Proc. IEEE Digital Signal Processing Workshop, Loen, Norway 9/1996.
10. J. B. Collins, Microwave Magnetrons, New York: McGraw-Hill, 1948.
11. J. Slater, Microwave Electronics, Princeton: Van Nostrand, 1950, (Particularly section 9.3).